

## CHAPTER 100

### Increased Dolos Strength by Shape Modification

S. A. Luger<sup>1</sup>, D. T. Phelp<sup>1</sup>, A. van Tonder<sup>1</sup> and A. H. Holtzhausen<sup>1</sup>

#### Abstract

A survey of prototype dolos breakages was performed to determine the distribution of failure modes. The results showed that 89% of the failures originate near the fluke-shank intersection. A series of static and dynamic finite element analyses was subsequently performed with the aim of improving the resistance of the dolos against the most commonly observed modes of failure. Of the six dolos shapes analysed, a large fillet extending from the fluke to the centre of the shank was found to be the most effective in reducing the stress in the critical fluke-shank intersection. Compared to a sharp intersection, the large fillet reduces the stress by more than 60%.

#### Introduction

A number of dolos-armoured breakwaters constructed in the 1960's and 1970's in South Africa now require repair work. This repair work generally involves placing additional layers of somewhat heavier dolosse on top of the damaged dolos slope.

A number of methods are available to improve the strength of these repair dolosse. These include an increase in waist ratio, the use of reinforcement (conventional, prestressed, rail or fibre) or a modification to the fluke-shank intersection. Increasing the waist ratio has the disadvantage of reducing the hydraulic stability (Holtzhausen and Zwamborn, 1992), while reinforcing increases the unit cost and there is

---

<sup>1</sup>Ematek, CSIR, P O Box 320, Stellenbosch 7599, South Africa

the potential for corrosion problems. In this paper the method of modifying the fluke-shank intersection is investigated. The initial phase of the study was to perform a survey of prototype dolos breakages. Various modifications to the fluke-shank intersection were then tested using static and dynamic finite element analysis.

### Survey of Prototype Dolos Breakages

The objective of the survey was to identify the main failure modes and determine the relative frequency of each mode. Use was made of close-range photographs taken from a crane on the breakwater crest or from a helicopter. Seven breakwaters were surveyed in this way and each of the 357 observed breakages were classified as one of six failure modes. The dolos masses ranged from 5 to 30 t and the waist ratios from 0,31 to 0,36. The fluke-shank intersections were either sharp or had a small fillet (radius approximately  $0,04H$ , where  $H$  is the dolos height) or a small chamfer (size approximately  $0,057H$ ).

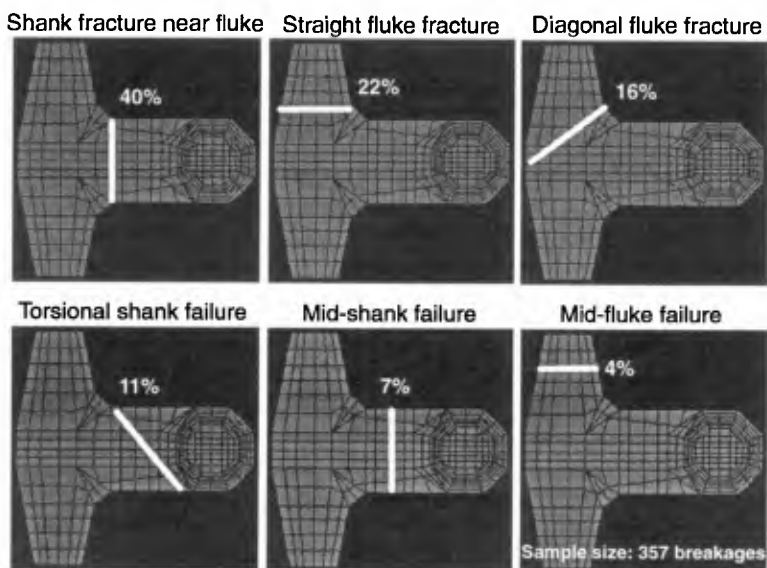


Figure 1. Distribution of prototype dolos failures

The six failure modes and the distribution of the failures are illustrated in Figure 1. The most common failure mode is a failure through the shank adjacent to a fluke. The four failure modes that originate near to the fluke-shank intersection account for 89% of the breakages.

The data set also indicated that dolosse with smaller waist ratios were more susceptible to failures through the shank. The dolosse with waist ratios of 0,31 had 86% shank failures and 14% fluke failures, while the dolosse with waist ratios of 0,34 to 0,36 had only 52% shank failures and 48% fluke failures. The chamfered or filleted units displayed proportionally more torsional failures (16% of all failures) than the dolosse with a sharp fluke-shank intersection (8% of all failures).

### Modifications to the Fluke-Shank Intersection

The original dolos shape had a sharp fluke-shank intersection (Merrifield and Zwamborn, 1966). Based on photo-elastic stress analysis Lillevang and Nickola (1976) suggested a fillet with a radius of  $0,04H$ , while Tait and Mills (1980) performed fatigue tests on model dolosse including one with a fillet radius of  $0,175H$ . The shape given in the Shore Protection Manual (CERC, 1984) has a chamfer with a dimension of  $0,057H$ . Rosson and Tedesco (1992) performed finite element simulations of the drop test using chamfer sizes of both  $0,06H$  and  $0,10H$ .

Based on the prototype breakages, it is expected that a stronger and more structurally-balanced dolos shape can be developed by further strengthening the fluke-shank intersection. Finite element models were therefore generated for six geometries of fluke-shank intersection. Each model had approximately 1900 quadratic elements and 8500 nodes. The six meshes are illustrated in Figure 2.

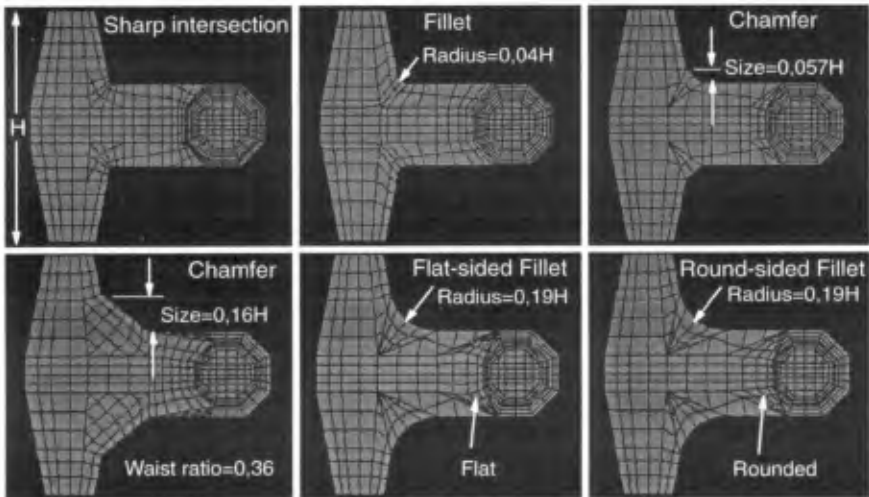


Figure 2. Shapes modelled in F E analyses

The top three shapes in Figure 2 are existing designs representative of the broken prototype dolosse analysed above. The bottom three shapes are new shapes aimed at strengthening the fluke-shank intersection. The dolosse all have a waist ratio of 0,36 while the height (H) was varied to ensure that all shapes had the same mass. The large chamfer extends to the middle of the shank and the angle between the chamfer and the shank is equal to the angle between the chamfer and the fluke. This gives a chamfer size of approximately 0,16H at a waist ratio of 0,36. The large fillet also extends to the middle of the shank which results in a radius of approximately 0,19H at a waist ratio of 0,36. Two different shapes incorporating the large fillet were tested. For the first shape the sides of the fillet consist of flat surfaces while for the second shape the sides of the fillet are rounded to intersect the shank and fluke smoothly.

### Static Finite Element Analyses

A series of static finite element analyses was performed in order to compare the maximum principal tensile stresses for each of the six dolos shapes. Linear elastic material behaviour was assumed and the results are thus only applicable up to the initiation of cracking. The following material properties were used: Density 2400 kg/m<sup>3</sup>, Young's modulus 27 GPa, Poisson's ratio 0,17.

The loading and boundary conditions applying to dolosse on a breakwater are extremely varied and complex and cannot therefore be reproduced in a deterministic finite element analysis. Only three simplified loading conditions (Figure 3) were analysed. The hanging load case was assumed to represent the shank fractures near to a fluke (40% of prototype fractures - refer to Figure 1). The fluke load represents the straight and diagonal fluke fractures (38% of prototype fractures) while the torsional load represents the torsional shank failures (11% of prototype fractures).

The surface stress distributions for the six dolos shapes due to the hanging load case are shown in Figure 4. The stress concentration in the sharp intersection can clearly be seen. The larger 0,16H chamfer does not reduce the stress compared to the 0,057H chamfer, due to the stiffer response of the larger chamfer. The lowest stress occurs for the 0,19H fillet with flat sides, due to the fact that this shape results in a slightly wider fillet than the 0,19H fillet with rounded sides. The torsional plots (Figure 5) show that the 0,16H chamfer again performs poorly. The 0,19H fillet with rounded sides shows the lowest stress. The 0,19H fillet with flat sides has a relatively sharp intersection between the flat sides and the shank which increases the stress in this area.

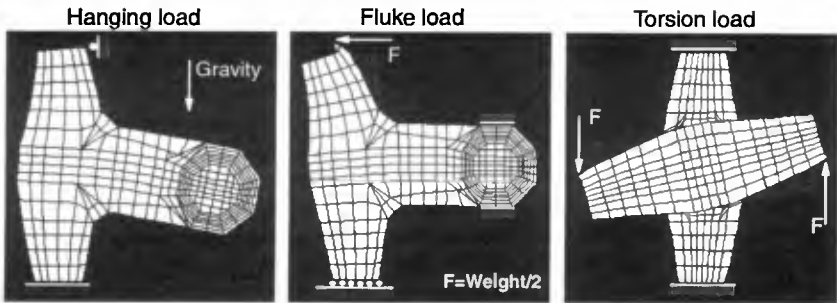


Figure 3. Static load cases

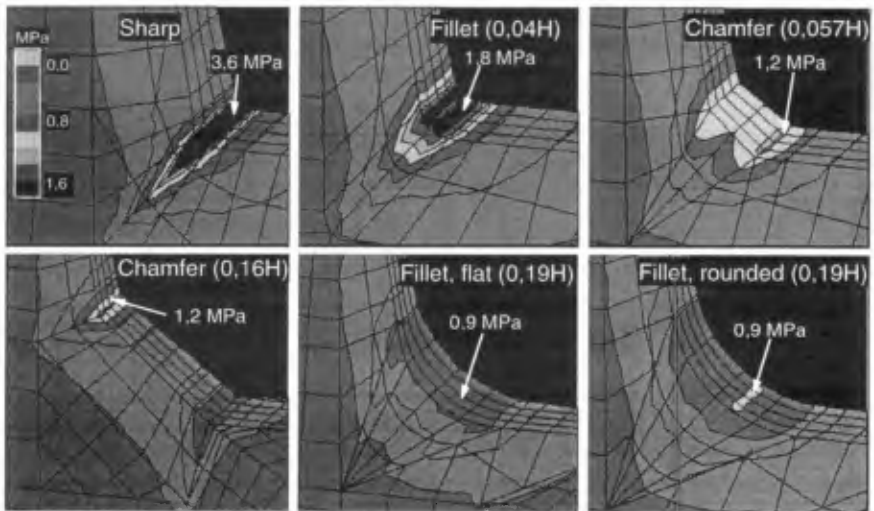


Figure 4. Principal tensile stresses - Hanging load case

Stress reduction factors were determined for each shape relative to the sharp intersection. These reduction factors were then weighted based on the relative frequency of each failure mode. 11% of the prototype failures occurred away from the fluke-shank intersection and this weighting was therefore applied to all the shapes. The results are summarised in Table 1.

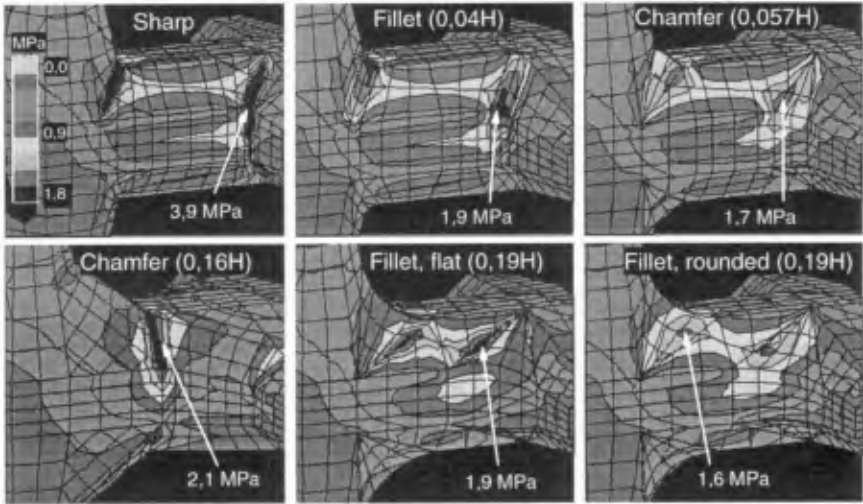


Figure 5. Principal tensile stresses - Torsional load case

	Load case	Geometry of fluke-shenk intersection					
		Sherp	Fillet (0,04H)	Chemfer (0,057H)	Chamfer (0,16H)	Fillet,flat (0,19H)	Fillet,round (0,19H)
Stress reduction factor relative to sherp shape	Shenk	1,00	0,51	0,33	0,34	0,24	0,26
	Fluke	1,00	0,52	0,38	0,47	0,29	0,30
	Torsion	1,00	0,49	0,44	0,52	0,49	0,41
Weighted reduction factor (weighting in brackets)	Shank (0,40)	0,40	0,20	0,13	0,14	0,09	0,10
	Fluke (0,38)	0,38	0,20	0,15	0,18	0,11	0,11
	Torsion (0,11)	0,11	0,05	0,05	0,06	0,05	0,04
	Other (0,11)	0,11	0,11	0,11	0,11	0,11	0,11
Total reduction factor	All	1,00	0,56	0,44	0,48	0,37	0,37

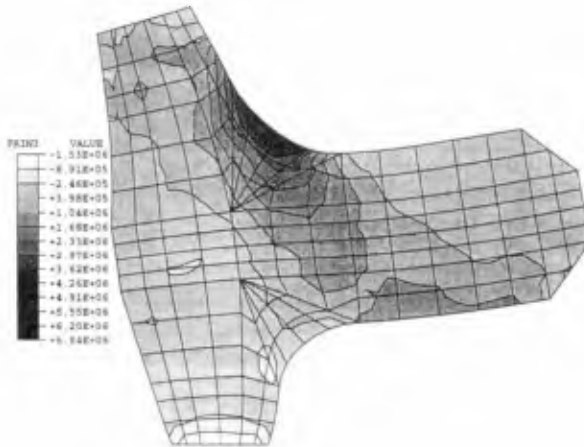
Table 1: Stress reduction factors for static loading

The two 0,19H fillet shapes show total static reduction factors of 0,37 compared to the sharp shape, 0,66 compared to the 0,04H fillet and 0,84 compared to the 0,057H fillet. In general, these modifications to the fluke-shank intersection do not reduce the torsional stresses as significantly as the stresses due to the hanging and fluke loads. This corresponds to the prototype breakages, where fillets or chamfers were found to increase the relative proportion of torsional failures.

**Dynamic Finite Element Analyses**

The response of the six dolos shapes to dynamic impact loading was also compared. The load case selected was the drop test (Burcharth, 1981). The material was modelled as linear elastic and no yield of the impacted surface was allowed. The implicit method of time integration was used with a constant time step of 5  $\mu$ s, which is approximately a quarter of the time required for a stress wave to travel between the integration points in an element.

The maximum principal tensile stresses occurred at the fluke-shank intersection, as illustrated in Figure 6. The computed stress reduction factors relative to the sharp intersection are presented in Table 2. These factors are similar to those computed for the static loads.



1,1 ms after impact, magnification factor = 1000

**Figure 6. Tensile stress distribution during drop test.**

	Geometry of fluke-shank intersection					
	Sharp	Fillet (0,04H)	Chamfer (0,057H)	Chamfer (0,16H)	Fillet,flat (0,19H)	Fillet,round (0,19H)
Drop test reduction factor	1,00	0,54	0,45	0,51	0,32	0,34

**Table 2: Stress reduction factors for dynamic loading**

## Conclusions

89% of prototype dolos breakages were found to occur near to the fluke-shank intersection. The static and dynamic tensile stresses at the fluke-shank intersection can be reduced by more than 60% by incorporating a large fillet extending to mid-shank. Although little difference in performance was found between the flat-sided and the round-sided fillet, the round-sided fillet is preferred due to its superior torsion resistance.

## Applications and Future Developments

The 0,19H fillet with round sides is being used for the repair of a number of breakwaters; the dolos sizes range from 7,5 to 30 t. A series of prototype drop tests has also been performed using 7,5 t dolosse with different fluke-shank intersections.

An aspect that has not been tested is the influence of the 0,19H fillet on the hydraulic stability of the dolos. A comparison between the profile of this shape and the 0,057H chamfer does reveal a large difference - the effect on the interlocking is thus expected to be small. This assumption must, however, still be tested by means of physical model studies.

## References

- Burcharth, H F (1981). Full-scale dynamic testing of dolosse to destruction. *Coastal Engineering Vol 4 No 3*.
- CERC (1984). *Shore Protection Manual*. US Army Coastal Engineering Research Center. US Government Printing Office, Washington DC.
- Holtzhausen, A H and Zwamborn, J A (1992). New stability formula for dolosse. *Proc 23rd ICCE*. Venice, Italy.
- Lillevang, O J and Nickola, W E (1976). Experimental studies of stresses within the breakwater armour piece "Dolos". *Proc 15th ICCE*. Honolulu, Hawaii.
- Merrifield, E M and Zwamborn, J A (1966). The economic value of a new breakwater armour unit "Dolos". *Coastal Engineering Vol 11*.

Rosson, B T and Tedesco, J w (1992). Dynamic response of dolos armour units to drop test impact loads. *Ocean engineering, Vol 19 No 6.*

Tait, R B and Mills, R D (1980). An investigation into the material limitations of breakwater dolosse. *ECOR Newsletter No 12.* Stellenbosch.